

Article

Analysis of Commercial Proanthocyanidins. Part 6: Sulfitation of Flavan-3-Ols Catechin and Epicatechin, and Procyanidin B-3

Anwar E. M. Noreljaleel, Anke Wilhelm  and Susan L. Bonnet *

Department of Chemistry, University of Free State, Bloemfontein 9301, South Africa; anwarelbushra@yahoo.ca (A.E.M.N.); WilhelmA@ufs.ac.za (A.W.)

* Correspondence: BonnetSL@ufs.ac.za; Tel.: +27-51-401-3018

Academic Editors: Teresa Escribano-Bailón and Ignacio García-Estévez

Received: 11 September 2020; Accepted: 13 October 2020; Published: 28 October 2020



Abstract: Proanthocyanidins (PACs) are natural plant-derived polymers consisting of flavan-3-ol monomers. Quebracho (*Schinopsis lorentzii* and *balansae*) heartwood and mimosa (*Acacia mearnsii*) bark extracts are the major industrial sources of PACs. These commercial extracts are often sulfited to reduce their viscosity and increase their solubility in water. The chemical process of sulfitation is still poorly understood regarding stereochemical influences during the reaction and during the cleavage of the interflavanyl bond of oligomers. To gain a better understanding of sulfitation, two diastereomeric flavan-3-ol monomers were sulfited under industrial conditions, and procyanidin B-3 (catechin-4 α - \rightarrow -8-catechin) were sulfited to investigate interflavanyl bond cleavage with sulfitation at C-4. Treatment of diastereomeric flavan-3-ols 2R,3S-catechin and 2R,3R-epicatechin with NaHSO₃ at 100 °C in aqueous medium afforded the enantiomeric (1R,2S)- and (1S,2R)-1-(3,4-dihydroxyphenyl)-2-hydroxy-3-(2,4,6-trihydroxyphenyl)propane-1-sulfonic acid, respectively. Utilizing computational NMR PD4 calculations it was determined that the direction of stereoselective nucleophilic attack is controlled by the C-3 configuration of the flavan-3-ols catechin and epicatechin. Sulfitation of the catechin-4 α - \rightarrow -8-catechin dimer 7 (procyanidin B-3) under the same conditions led to the cleavage of the interflavanyl bond yielding the C-4 sulfonic acid substituted catechin monomer. From the heterocyclic ring coupling constants it was determined that nucleophilic attack occurs from the β -face of the dimer leading to the 2,3-*trans*-3,4-*cis* isomer as product.

Keywords: sulfitation; tannins; *Acacia mearnsii* de Wild.; flavan-3-ol, C-2 sulfonation; PD4 calculations; procyanidin B-3; C-4 sulfonation

1. Introduction

The tanning of animal skins or hides into durable leather has been practiced since antiquity, and the original method used was vegetable pit tanning [1]. Vegetable material containing tannins reacts irreversibly with the protein constituents of hides to yield soft leather, which is resistant to microbial degradation, water, heat and abrasion [2]. Tannins are secondary metabolites found in higher plants and mainly consist of hydrolysable tannins (polyesters of gallic or hexahydroxydiphenic acid and D-glucose) and proanthocyanidins (PACs), also known as condensed tannins (complex oligomers of flavan-3-ol monomers) (Figure 1). The four major trees from which tanning material is extracted are mimosa (*Acacia mearnsii* bark) and quebracho (*Schinopsis lorentzii* and *S. balansae*, heartwood) for condensed tannins [3,4] and chestnut (*Castanea sativa* and *C. dentate*, wood) [5] and tara (*Caesalpinia spinosa*, pods) for hydrolysable tannins [6].

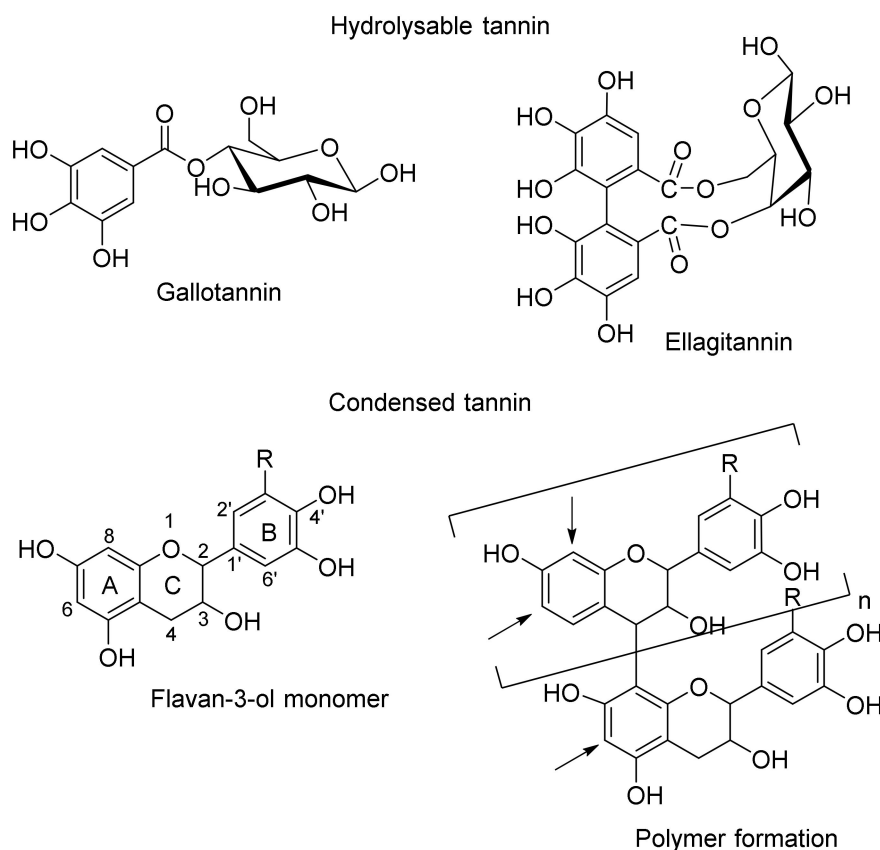


Figure 1. Basic structures of hydrolysable and condensed tannins.

Hydrogen bond formation between the hydroxy groups of the polyphenolic PACs and proteins forms the basis for many of the tannin extract applications. In plants the formation of indigestible PAC-protein complexes gives rise to the anti-feeding effect and protects the plants from herbivores [7]. Industrially, PAC extracts are still widely used in the leather industry [8], the adhesive industry [9], as additives to animal feed [10], the wine industry [11], as flocculants [12–14], and as mud-drilling additives [13]. Pharmacological properties include anti-oxidant activity [15–17], Alzheimer’s disease inhibition [18], anti-cancer activity [19,20], anti-diabetic [21,22], anti-microbial [23,24] and anti-cardiovascular diseases [25,26].

Tannins have been chemically modified for the development of new biobased polymers to enhance industrial applications. The main sites on the condensed tannin structure for modifications are the phenolic hydroxy groups (etherification and esterification [27,28]), opening of the heterocyclic ring with substitution at C-2 (e.g., sulfitation [29]), electrophilic aromatic substitution on mainly the more reactive A-ring at positions 6 and 8 (e.g., bromination [30,31]), condensation reactions [32], reactions with aldehydes leading to polymerization via methylene bridges [33] and methylamination via the Mannich reaction [30,34,35].

The sulfitation of condensed tannins is one of the oldest modification reactions and changes the physical and chemical properties of PAC extracts. The reaction greatly improves the water solubility of PACs and also reduces the viscosity of PAC extracts [30]. Furthermore, the moisture retention of tannin adhesives is enhanced and consequently the adhesive film dries more gradually [29]. During sulfitation the heterocyclic C-ring of the flavan-3-ol monomer building block is cleaved, affording sulfonic acid derivatives [29,36], and secondly, the interflavanyl bond between two flavan-3-ol units can be cleaved. Extensive studies on the composition of the unsulfited and sulfited PAC extracts from quebracho heartwood and black wattle bark via low and high resolution electron spray ionization mass spectrometry (LR-ESIMS and HR-ESIMS) supported these findings [37–40]. They concluded that the flavan-3-ol building blocks of quebracho heartwood PACs were catechin as starter unit and fisetinidol

as extender unit [37], while PACs in black wattle bark extract comprise catechin and gallo catechin starter units, and fisetinidol and robinetinidol extender units [39] (Figure 2).

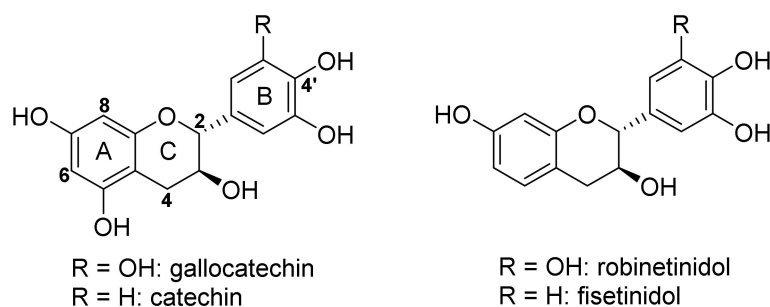


Figure 2. Flavan-3-ol monomers isolated from *Acacia mearnsii* De Wild. bark.

Sulfitation of the quebracho PACs thus transforms the hot-water-soluble extract into a cold-water-soluble extract, since the introduction of sulfonic acid moieties increases the polarity of the molecules [38]. They also reported that no sulfitation at the C-4 positions of the starter units catechin and gallo catechin was observed, but that interflavanyl bond cleavage affords sulfitation at C-4 of the extender units, shortening chain lengths [37–40]. They thus deduced that C-4 sulfitation only occurs on the extender units (Figure 3).

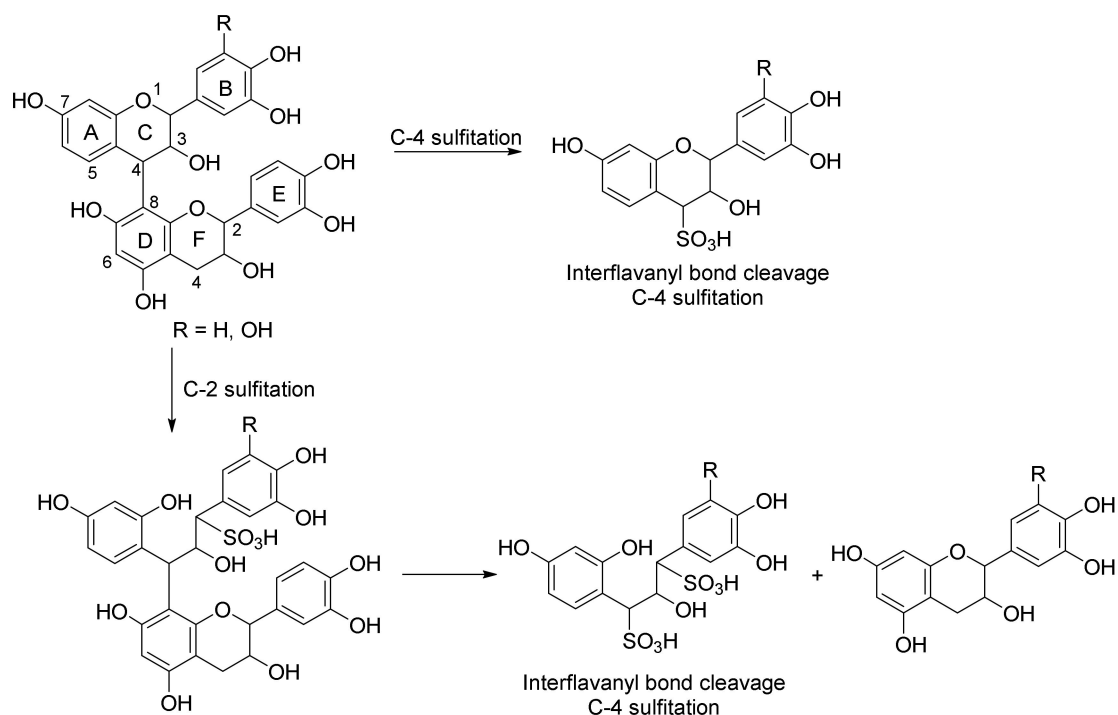


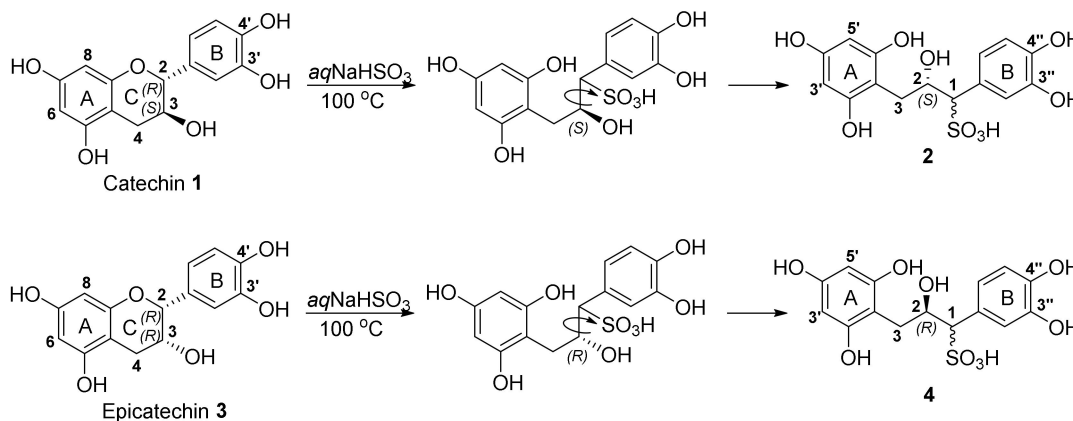
Figure 3. Sulfitation of a PAC dimer affords C-2 and C-4 (interflavanyl bond fission) sulfonated products.

However, even though sulfitation of tannin structures is a well-known reaction, the chemical process of sulfitation is still poorly understood regarding stereochemical influences during the reaction and the cleavage of the interflavanyl bond of oligomers. To gain a better understanding of sulfitation, two diastereomeric flavan-3-ol monomers were sulfited under industrial conditions, and procyanidin B-3 (catechin-4 α -8-catechin) were sulfited to investigate interflavanyl bond cleavage.

2. Results and Discussion

2.1. Sulfitation of Diastereomeric 2*R*,3*S*-Catechin and 2*R*,3*R*-Epicatechin

Treatment of diastereomeric flavan-3-ols 2*R*,3*S*-catechin (**1**) and 2*R*,3*R*-epicatechin (**3**), respectively, with NaHSO₃ at 100 °C in aqueous medium afforded only one major ring-opened product in each reaction, **2** and **4**, respectively, with a sulfonic acid group at C-1 (Scheme 1).

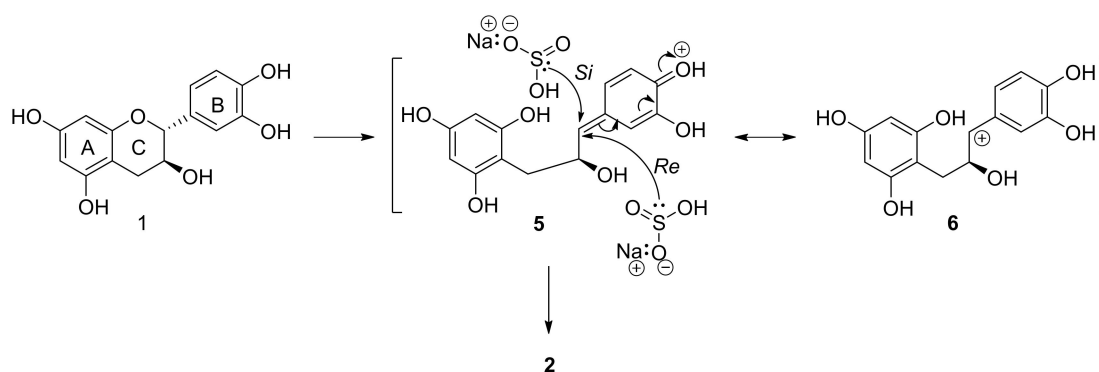


Scheme 1. Sulfitation of 2*R*,3*S*-catechin **1** and 2*R*,3*R*-epicatechin **3**.

During structure elucidation it was observed that products **2** and **4** had identical ¹H and ¹³C NMR spectra, but opposite Cotton effect electron circular dichroism (ECD) spectra, indicating an enantiomeric relationship between **2** and **4**. The aromatic region of the ¹H NMR spectra of enantiomers **2** and **4** show one two-proton singlet at δ_H 5.87 and 5.88, respectively, corresponding to the equivalent H-3' and H-5' of the free-rotating phloroglucinol A-ring, and one ABX system corresponding to the B-ring at δ_H 6.75 and 6.76 (d, H-5'') and 6.78 and 6.79 (dd, H-6''), respectively, and 6.95 (d, H-2'') for both **2** and **4**. In the aliphatic region, H-1 is observed at δ_H 3.81 as a triplet of doublets, H-2, situated on the oxygenated C-2, at δ_H 4.53, and H-3_{eq} and H-3_{ax} is observed as two doublet of doublets at δ_H 2.79 and 2.45, respectively.

Owing to free rotation about aliphatic bonds, the absolute configuration at C-1 of **2** and **4** cannot be determined via aliphatic coupling constants in the ¹H NMR spectra. However, the enantiomeric relationship implies that the absolute configuration at C-1 of the products are determined by the absolute configuration at the C-3 chiral center of the starting materials. It has been postulated that cleavage of the heterocyclic C-ring of **1** and **3** can result in two possible tautomeric intermediates [41]: either the *para*-quinone methide of the B-ring (**5**), or the *para*-hydroxy stabilized benzylic cation (**6**) (Scheme 2). They further reported that the hydroxy-group at C-4' is essential for substitution at C-2 of the starting materials. Both tautomeric intermediates **5** and **6** are planar, due to sp²-hybridization of C-1, and nucleophilic attack can thus occur either on the *Si*-face or the *Re*-face of the intermediates (Scheme 2).

The absolute configuration at C-1 of the sulfonic acid adduct depends on the face of attack at the planar C-1 center in the tautomeric intermediates. Attack on the *Si*-face will afford 1*S* absolute configuration at C-1, while *Re*-face attack will give rise to 1*R* absolute configuration. Stereoselective attack can be directed by either the benzyl group or the hydroxy group at C-2, dependent on the preferred conformation of the aliphatic system. Bach and coworkers postulated that α-chiral secondary and tertiary benzylic carbocations have a preferred conformation where the α-hydrogen atom occupies the 1,3-allylic strain position (Figure 4) [42].



Scheme 2. Proposed mechanism of the sulfitation of catechin 1.

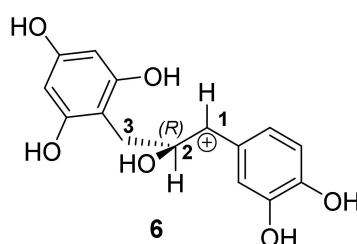
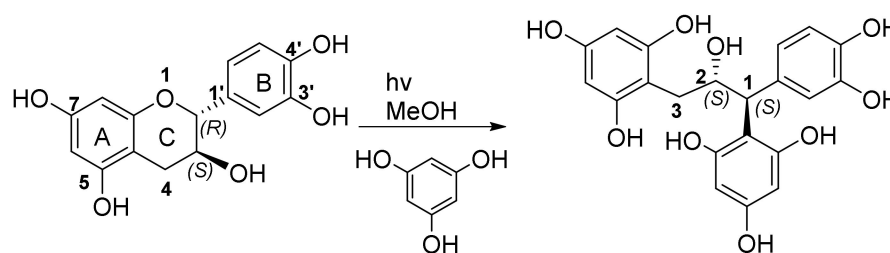


Figure 4. Most stable conformation of the benzylic carbocation intermediate (6) with the α -H in the 1,3-allylic strain position.

Diastereotopic faces of carbocations are differentiated by the functional groups at the α -carbon.

In the case of intermediate 6, this would imply that the bulkier benzyl group at C-2 and not the less bulky hydroxy group at C-2 will direct attack to the *Si*-face leading to the 1*S*,2*S* diastereomer. However, Wilhelm and co-workers [41] cleaved the heterocyclic ring of flavan-3-ols (catechin and epicatechin, respectively) via photolytic fission of the ether bond. Trapping of the intermediates with phloroglucinol afforded phloroglucinol-grafted derivatives, with identical NMR spectra indicating formation of enantiomers. In this case the C-2 absolute configuration was established via theoretical calculation of the electronic circular dichroism (ECD) spectra. The results indicated that the hydroxy group at C-3 directed attack to the *Re*-face leading to the 1*S*,2*S* diastereomer (Scheme 3).



Scheme 3. Photolysis of catechin in the presence of phloroglucinol.

In order to unequivocally determine the absolute configuration at C-1 of products 2 and 4, gauge-invariant atomic orbital (GIAO) NMR shift calculation and DP4 (isomer probability parameter) analysis were performed.

2.2. GIAO NMR Shift Calculation and DP4 Analysis

Computational NMR prediction has become a common tool to calculate theoretical NMR shifts [43,44]. Smith and Goodman used gauge-invariant atomic orbital (GIAO) NMR shift calculations to determine stereochemistry in several pairs of diastereomers [45]. They subsequently applied GIAO NMR shift

calculations to assign stereochemistry with quantifiable confidence when only one set of experimental data was available, formulating and applying the DP4 parameter, which aids in assigning structure and stereochemistry by comparing experimental and calculated NMR spectra [46]. The only requirements for this process are the experimentally defined ^1H and ^{13}C NMR chemical shifts. It involves the calculation of the shifts for the candidate structures (employing a Boltzmann weighted average of the shifts calculated for all low-energy conformers), followed by DP4 comparison to the experimental data to decide which gives the best match. The program also gives a measure of its confidence in its conclusion.

Thus, the calculated and experimental NMR data depicted in Table S1 and Table S2 were determined via GIAO NMR shift calculation and DP4 analysis of our proposed structures **2** and **4**, and the absolute configurations were indicated to be 1*R*,2*S* for **2** and 1*S*,2*R* for **4** with 100% confidence (Figure 5 and Table 1).

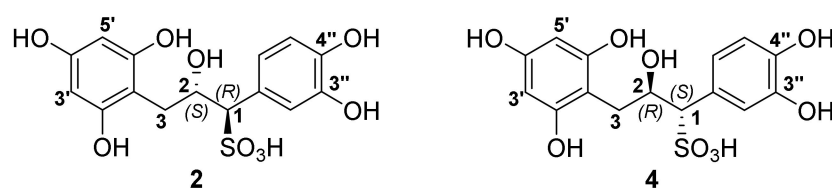


Figure 5. Absolute configurations of sulfited catechin (**2**) and sulfited epicatechin (**4**).

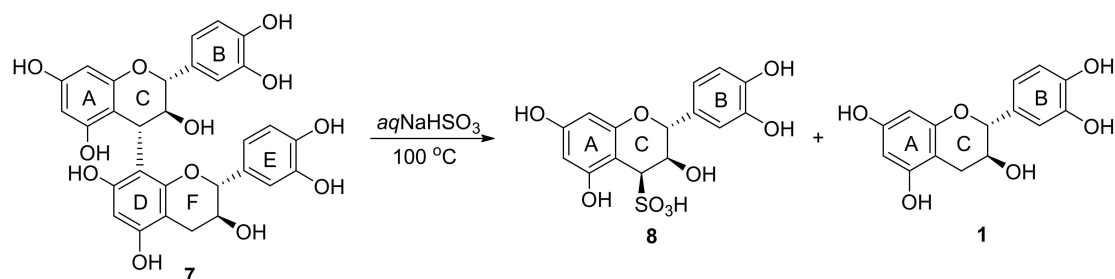
Table 1. DP4 probability results for products **2** and **4**.

| Probability | Sulfited Catechin (2) | | Sulfited Epicatechin (4) | |
|---------------------|--------------------------------|-----------------------|-----------------------------------|-----------------------|
| | 1 <i>R</i> 2 <i>S</i> | 1 <i>S</i> 2 <i>S</i> | 1 <i>R</i> 2 <i>R</i> | 1 <i>S</i> 2 <i>R</i> |
| ^1H NMR | 99.7% | 0.3% | 2.3% | 97.7% |
| ^{13}C NMR | 96.1% | 3.9% | 38.9% | 61.1% |
| Combined | 100.0% | 0% | 0% | 100.0% |

Thus, stereoselective attack leads to the formation of enantiomeric products when catechin and epicatechin are sulfonated. The direction of nucleophilic attack is controlled by the C-3 configuration of the flavan-3-ols **1** and **3**. In the case of the catechin intermediate **5/6**, *Re*-face attack afforded (1*R*,2*S*)-1-(3,4-dihydroxyphenyl)-2-hydroxy-3-(2,4,6-trihydroxyphenyl)propane-1-sulfonic acid (**2**), and for epicatechin *Si*-face attack yielded (1*S*,2*R*)-1-(3,4-dihydroxyphenyl)-2-hydroxy-3-(2,4,6-trihydroxyphenyl)propane-1-sulfonic acid (**4**).

2.3. Sulfitation of Procyanidin B-3

Sulfitation of the catechin-4 α - \rightarrow 8-catechin dimer **7** (procyanidin B-3) under the same conditions led to the cleavage of the interflavanyl bond yielding the C-4 sulfonic acid substituted monomer **8** and **1** (Scheme 4).



Scheme 4. Sulfitation of procyanidin-B3.

The aromatic region of the ^1H NMR spectrum indicated two doublets corresponding to the A-ring protons at δ_{H} 5.95 (H-6) and 6.04 (H-8) and an aromatic ABX system at δ_{H} 6.96 (H-2', d), 6.81 (H-5', d) and 6.83 (H-6', dd). The heterocyclic ring protons resonated at δ_{H} 5.53 (H-2, d), δ_{H} 4.13 (H-3, dd) and δ_{H} 4.52 (H-4, d). Van der Westhuizen et al. used the ^1H NMR coupling constants of the C-ring resonances to distinguish between the diastereoisomers of 4-arylflavan-3-ols [47]. The characteristic coupling constants for 4-arylflavan-3-ols with a 2,3-*trans*-3,4-*cis* relative stereochemistry are $J_{2,3} = 8\text{--}10$ Hz and $J_{3,4} = 5.0\text{--}6.5$ Hz. Extrapolating to our 4-substituted flavan-3-ols, the coupling constants of $J_{2,3} = 10.3$ Hz and $J_{3,4} = 5.1$ Hz for **11** indicates a 3,4-*cis* relative stereochemistry, thus the absolute configuration at C-4 is 4S (Figure 1). This indicates that nucleophilic attack occurs selectively from the β -face of the heterocyclic ring, as expected, since the large C-4 substituent is blocking the α -face of the dimer. The cleavage of the interflavanyl bond in condensed tannin extracts leads to smaller oligomers that may be beneficial for leather tanning, since the preferable chain length for leather bonding is three to four monomers.

3. Conclusions

Treatment of the two diastereomeric flavan-3-ol monomers catechin and epicatechin, with NaHSO_3 at 100°C in aqueous medium, yielded sulfited enantiomeric products, which confirmed our previous findings [40] that sulfonic acid moieties ($-\text{SO}_3\text{H}$) are stereoselectively introduced at C-2, with cleavage of the ether bond of the heterocyclic C-ring. It was demonstrated, via GIAO NMR shift calculations and DP4 analysis, that the stereochemistry at C-1 of the formed sulfited products is controlled by the C-3 configuration of the starting flavan-3-ols. Sulfitation of the catechin-4 α →8-catechin dimer (procyanidin B-3) under the same conditions led to the cleavage of the interflavanyl bond yielding the 2,3-*trans*-3,4-*cis* C-4 sulfonic acid substituted monomer, exclusively. This finding substantiates our previous results [40] that cleavage of the interflavanyl bond leads to shorter chain lengths that contribute to the reduced viscosity, improved solubility and better raw skin penetration of sulfited wattle bark extract.

4. Materials and Methods

Chemicals purchased from commercial vendors were reagent/analytical grade and were used without purification. Catechin, epicatechin and sodium hydrogen sulfite were purchased from Sigma-Aldrich (Johannesburg, South Africa). Procyanidin B-3 was synthesized in-house and purity determined via HPLC. Solvents methanol, hexane and ethyl acetate were purchased from Merck (Johannesburg, South Africa).

A 600 MHz Bruker Avance II NMR spectrometer with a ^{13}C and ^1H 5 mm DUAL ^{13}C - $^1\text{H}/\text{D}$ probe with z-gradients operating at 25°C was used to record all NMR spectra at a ^1H frequency of 600.28 MHz and a ^{13}C frequency of 150.95 MHz. The instrument was manufactured by Bruker Biospin AG at Fällanden, Switzerland. The ^1H NMR, COSY, HMBC, HSQC, ^{13}C and APT experiments were performed in methanol- d_4 , ($\delta_{\text{H}} = 4.87$ and 3.31 ; $\delta_{\text{C}} = 49.2$) with tetramethylsilane (TMS) as internal standard. Chemical shifts were expressed as parts per million (ppm) on the delta (δ) scale and coupling constants (J) are accurate to 0.01 Hz.

Thin-layer chromatography (TLC) was performed on Merck aluminium sheets (silica gel 60 F₂₅₄, 0.25 mm). Reactions were monitored using TLC on silica gel, with detection by UV light (254 nm). Thin-layer chromatograms were sprayed with a 2% (*v/v*) solution of formaldehyde (40% solution in water) in concentrated sulphuric acid and subsequently heated to 110°C to effect maximum development of colour.

All conformational searches were conducted employing the MacroModel (Version 9.9, Schrodinger LLC., New York, NY, USA) program with "Mixed torsional/LowMode sampling" in the MMFF force field. The searches were performed in the gas phase with a 50 kJ/mol energy window limit and 10,000 maximum number of steps to fully explore all low-energy conformers. All minimization processes were carried out utilizing the Polak-Ribiere conjugate gradient (PRCG) method, 10,000

maximum iterations and a 0.001 convergence threshold. The GIAO shielding constants of all conformers within 10 kJ/mol of the global minimum were calculated utilizing a Gaussian 09 package (Gaussian Inc., Wallingford, CT, USA) at the B3LYP/6-31G(d,p) level in the gas phase. The calculation of DP4 probability was facilitated using an applet available at "<http://www-jmg.ch.cam.ac.uk/tools/nmr/DP4/T1/textquotedblright>."

General procedure for sulfitation:

The flavan-3-ol (or dimer) (100 mg), excess sodium hydrogen sulfite (100 mg) and water (4 mL) were sealed in a glass tube and heated at 100 °C for 8 h. The reaction mixture was cooled down, extracted with ethyl acetate (2 × 20 mL) to remove unreacted catechin and the water layer lyophilized. The crude was subsequently dissolved in methanol, the unreacted NaHSO₃ filtered off and the solvent removed under vacuum to yield the amorphous product.

NMR data of all the products are available in the Supplementary Materials section, Table S1–S3.

Supplementary Materials: The following are available online at <http://www.mdpi.com/1420-3049/25/21/4980/s1>, Table S1: Experimental and calculated ¹H and ¹³C NMR shifts for compound **2**, Table S2: Experimental and calculated ¹H and ¹³C NMR shifts for compound **4**, Table S3: ¹H (600 MHz, MeOD, 20 °C) and ¹³C NMR data (150 MHz, CD₃OD, 20 °C) of 2R,3R,4S-catechin-4β-sulfonic acid (**8**). Figure S1: ¹H NMR of sulfited catechin **2**, Figure S2: ¹³C NMR of sulfited catechin **2**, Figure S3: ¹H NMR of sulfited epicatechin **4**, Figure S4: ¹³C NMR of sulfited epicatechin **4**, Figure S5: ¹H NMR of C-4 sulfited catechin **8**.

Author Contributions: Conceptualization, S.L.B.; methodology, S.L.B. and A.E.M.N.; formal analysis, A.E.M.N.; investigation, A.E.M.N.; supervision, S.L.B.; writing—original draft preparation, A.E.M.N. and S.L.B.; writing—review and editing, A.W.; project administration, S.L.B. All authors have read and agreed to the published version of the manuscript.

Funding: This research received no external funding.

Acknowledgments: We hereby acknowledge Oh, J. (Yale University, USA) and Geny, C. (Natural Product Chemistry Institute, Paris, France) for the performance of the GIAO NMR DP4 calculations.

Conflicts of Interest: The authors declare no conflict of interest.

References

1. Covington, A.D. *Tanning Chemistry: The Science of Leather*; Royal Society of Chemistry: Cambridge, UK, 2009; ISBN 978-1-84973-434-9.
2. Haslam, E. Polyphenols, collagen and leather. In *Practical Polyphenolics. From Structure to Molecular Recognition and Physiological Action*; Cambridge University Press: Cambridge, UK, 2005; p. 378.
3. Roux, D.G.; Paulus, E. Condensed tannins. 12. Polymeric leucofisetinidin tannins from the heartwood of *Acacia mearnsii*. *Biochem. J.* **1962**, *82*, 320–324. [[CrossRef](#)]
4. Roux, D.G.; Evelyn, S.R. Condensed tannins 2. Biogenesis of condensed tannins based on leucoanthocyanins. *Biochem. J.* **1958**, *70*, 344–349. [[CrossRef](#)] [[PubMed](#)]
5. Robert, W.; Griffith, R.W. Chestnut wood in the tanning industry. *J. For.* **1924**, *22*, 542–545. [[CrossRef](#)]
6. Garro Galvez, J.M.; Riedl, B.; Conner, A.H. Analytical studies on tara tannins. *Holzforschung* **1977**, *51*, 235–243. [[CrossRef](#)]
7. Cooper, S.M.; Owen-Smith, N.; Bryant, J.P. Foliage acceptability to browsing ruminants in relation to seasonal changes in the leaf chemistry of woody plants in a South African savanna. *Oecologia* **1988**, *75*, 336–342. [[CrossRef](#)] [[PubMed](#)]
8. Ismail, A.R.; Mohd Norddin, M.N.A.; Latefi, N.A.S.; Oseh, J.O.; Ismail, I.; Gbadamosi, A.O.; Agi, A.J. Evaluation of a naturally derived tannin extracts biopolymer additive in drilling muds for high-temperature well applications. *J. Petrol Explor. Prod. Technol.* **2020**, *10*, 623–639. [[CrossRef](#)]
9. Pizzi, A. Hot-setting tannin-urea-formaldehyde exterior wood adhesives. *Adhes. Age* **1977**, *20*, 27–29.
10. Waghorn, G. Beneficial and detrimental effects of dietary condensed tannins for sustainable sheep and goat production: Progress and challenges. *Anim. Feed Sci. Technol.* **2008**, *147*, 116–139. [[CrossRef](#)]
11. Parker, M.; Smith, P.A.; Birse, M.; Francis, I.L.; Kwiatkowski, M.J.; Lattey, K.A.; Liebich, B.; Herderich, M.J.L. The effect of pre- and post-ferment additions of grape derived tannin on Shiraz wine sensory properties and phenolic composition. *Aust. J. Grape Wine R.* **2007**, *13*, 30–37. [[CrossRef](#)]

12. Beltran-Heredia, J.; Sanchez-Martin, J. Removing heavy metals from polluted surface water with tannin-based flocculant agent. *J. Hazard. Mater.* **2008**, *165*, 1215–1218. [[CrossRef](#)]
13. Beltran-Heredia, J.; Sanchez-Martin, J. Municipal wastewater treatment by modified tannin flocculent agent. *Desalination* **2009**, *249*, 353–358. [[CrossRef](#)]
14. Beltran-Heredia, J.; Sanchez-Martin, J.; Frutos-Blanco, G. *Schinopsis balansae* tannin-based flocculant in removing dodecyl benzene sulfonate. *Sep. Purif. Technol.* **2009**, *67*, 295–303. [[CrossRef](#)]
15. Hagerman, A.E.; Riedl, K.M.; Rice, R.E. Tannins as Biological Antioxidants. In *Plant Polyphenols 2*; Gross, G.G., Hemingway, R.W., Yoshida, T., Branham, S.J., Eds.; Springer: Boston, MA, USA, 1999; Volume 66. [[CrossRef](#)]
16. Maisetta, G.; Batoni, G.; Caboni, P.; Esin, S.; Rinaldi, A.C.; Zucca, P. Tannin profile, antioxidant properties, and antimicrobial activity of extracts from two Mediterranean species of parasitic plant *Cytinus*. *BMC Complement. Altern. Med.* **2019**, *19*, 82. [[CrossRef](#)]
17. Koleckar, V.; Kubikova, K.; Rehakova, Z.; Kuca, K.; Jun, D.; Jahodar, L.; Opletal, L. Condensed and Hydrolysable Tannins as Antioxidants Influencing the Health. *Mini Rev. Med. Chem.* **2008**, *8*, 436. [[CrossRef](#)]
18. Gaudreault, R.; Mousseau, N. Mitigating Alzheimer's Disease with Natural Polyphenols: A Review. *Curr. Alzheimer Res.* **2020**, *16*, 529–543. [[CrossRef](#)]
19. Gollucke, A.P.; Aguiar, O., Jr.; Barbisan, L.F.; Ribeiro, D.A. Use of grape polyphenols against carcinogenesis: putative molecular mechanisms of action using in vitro and in vivo test systems. *J. Med. Food* **2013**, *16*, 199–205. [[CrossRef](#)] [[PubMed](#)]
20. Turati, F.; Rossi, M.; Pelucchi, C.; Levi, F.; la Vecchia, C. Fruit and vegetables and cancer risk: a review of southern European studies. *Br. J. Nutr.* **2015**, *113*, S102–S110. [[CrossRef](#)]
21. Gonzalez-Abuin, N.; Pinent, M.; Casanova-Marti, A.; Arola, L.; Blay, M.; Ardevol, A. Procyanidins and their healthy protective effects against type 2 diabetes. *Curr. Med. Chem.* **2015**, *22*, 39–50. [[CrossRef](#)]
22. Pinent, M.; Cedó, L.; Montagut, G.; Blay, M.; Ardévol, A. Procyanidins improve some disrupted glucose homeostatic situations: an analysis of doses and treatments according to different animal models. *Crit. Rev. Food. Sci. Nutr.* **2012**, *52*, 569–584. [[CrossRef](#)] [[PubMed](#)]
23. Marín, L.; Miguélez, E.M.; Villar, C.J.; Lombó, F. Bioavailability of dietary polyphenols and gut microbiota metabolism: antimicrobial properties. *Biomed. Res. Int.* **2015**, *2015*, 905215. [[CrossRef](#)]
24. Sieniawska, E. Activities of Tannins - From In Vitro Studies to Clinical Trials. *Nat. Prod. Commun.* **2015**, *10*, 1877–1884.
25. Mohana, T.; Navin, A.V.; Jamuna, S.; Sakeena Sadullah, M.S.; Niranjali Devaraj, S. Inhibition of differentiation of monocyte to macrophages in atherosclerosis by oligomeric proanthocyanidins -In-vivo and in-vitro study. *Food. Chem. Toxicol.* **2015**, *82*, 96–105. [[CrossRef](#)] [[PubMed](#)]
26. Holt, R.R.; Heiss, C.; Kelm, M.; Keen, C.L. The potential of flavanol and procyanidin intake to influence age-related vascular disease. *J. Nutr. Gerontol. Geriatr.* **2012**, *31*, 290–323. [[CrossRef](#)] [[PubMed](#)]
27. Alice Arbenz, A.; Avérous, L. Chemical modification of tannins to elaborate aromatic biobased macromolecular architectures. *Green Chem.* **2015**, *17*, 2626–2646. [[CrossRef](#)]
28. Nicollin, A.; Zhou, X.; Pizzi, A.; Grigsby, M.; Rode, K.; Delmotte, L. MALDI-TOF and ¹³C NMR analysis of a renewable resource additive—Thermoplastic acetylated tannins. *Ind. Crops Prod.* **2013**, *49*, 851–857. [[CrossRef](#)]
29. Pizzi, A. Sulfited tannins for exterior wood adhesives. *J. Org. Chem.* **1972**, *37*, 3546–3547.
30. Pizzi, A. Condensed tannins for adhesives. *Ind. Eng. Chem. Prod. Res. Dev.* **1982**, *21*, 359–369. [[CrossRef](#)]
31. Ferreira, D.; van Rensburg, H.; Malan, E.; Coetzee, J.; Nel, R.J.J. Recent Advances in the Chemistry of Proanthocyanidins. In *Phytochemicals in Human Health Protection, Nutrition, and Plant Defense. Recent Advances in Phytochemistry, Proceedings of the Phytochemical Society of North America*; Romeo, J., Ed.; Springer: Boston, MA, USA, 1999; Volume 33.
32. Viviers, P.M.; Kolodziej, H.; Young, D.A.; Ferreira, D.; Roux, D.G. Synthesis of condensed tannins. Part 11. Intramolecular enantiomerism of the constituent units of tannins from the Anacardiaceae: Stoichiometric control in direct synthesis: derivation of ¹H nuclear magnetic resonance parameters applicable to higher oligomers. *J. Chem. Soc. Perkin Trans. 1* **1983**, 2555–2562. [[CrossRef](#)]
33. Roux, D.G.; Ferreira, D.; Hundt, H.K.L.; Malan, E. Structure, stereochemistry, and reactivity of natural condensed tannins as basis for their extended industrial application. *Appl. Polym. Symp.* **1975**, *28*, 335–353.
34. Pizzi, A. Hardening mechanism of tannin adhesives with hexamine. *Holz Roh Werkst* **1994**, *52*, 229. [[CrossRef](#)]

35. Pizzi, A.; Kueny, R.; Lecoanet, F.; Massetau, B.; Carpentier, D.; Krebs, A.; Krebs, F.; Molina, S.; Ragoubi, M. High resin content natural matrix-natural fibre biocomposites. *Ind. Crops Prod.* **2009**, *30*, 235–240. [[CrossRef](#)]
36. Hoong, Y.; Paridaha, M.; Luqman, C.; Koh, M.; Loh, Y. Fortification of Sulfited Tannin from the Bark of Acacia mangium with Phenol-Formaldehyde for use as Plywood Adhesive. *Ind. Crops Prod.* **2009**, *30*, 416–421. [[CrossRef](#)]
37. Venter, P.B.; Sisa, M.; van der Merwe, M.J.; Bonnet, S.L.; van der Westhuizen, J.H. Analysis of commercial proanthocyanidins. Part 1: the chemical composition of quebracho (*Schinopsis lorentzii* and *Schinopsis balansae*) heartwood extract. *Phytochemistry* **2012**, *73*, 95–105. [[CrossRef](#)]
38. Venter, P.B.; Senekal, N.D.; Amra-Jordaan, M.; Bonnet, S.L.; van der Westhuizen, J.H. Analysis of commercial proanthocyanidins. Part 2: An electrospray mass spectrometry investigation into the chemical composition of sulfited quebracho (*Schinopsis lorentzii* and *Schinopsis balansae*) heartwood extract. *Phytochemistry* **2012**, *78*, 156–169. [[CrossRef](#)]
39. Venter, P.B.; Senekal, N.D.; Amra-Jordaan, M.; Bonnet, S.L.; Van der Westhuizen, J.H. Analysis of commercial proanthocyanidins. Part 3: The chemical composition of wattle (*Acacia mearnsii*) bark extract. *Phytochemistry* **2012**, *83*, 153–167. [[CrossRef](#)] [[PubMed](#)]
40. Noreljaleel, A.E.M.; Kemp, G.; Wilhelm, A.; van der Westhuizen, J.H.; Bonnet, S.L. Analysis of commercial proanthocyanidins. Part 5: A high resolution mass spectrometry investigation of the chemical composition of sulfited wattle (*Acacia mearnsii* De Wild.) bark extract. *Phytochemistry* **2019**, *162*, 109–120. [[CrossRef](#)]
41. Wilhelm-Mouton, A.; Bonnet, S.L.; Ding, Y.; Li, X.C.; Ferreira, D.; van der Westhuizen, J.H. Photochemistry synthesis. Part 2: Enantiomerically pure polyhydroxy-1,1,3-triarylpropan-2-ols. *J. Photochem. Photobiol. A Chem.* **2012**, *227*, 18–24. [[CrossRef](#)]
42. Stadler, D.; Goepfert, A.; Rasul, G.; Olag, G.A.; Surya Prakash, G.K.; Bach, T. Chiral benzylic carbocations: Low temperature NMR studies and theoretical calculations. *J. Org. Chem.* **2009**, *74*, 312–318. [[CrossRef](#)]
43. Barone, G.; Gomez-Paloma, L.; Duca, D.; Silvestri, A.; Riccio, R.; Bifulco, G. Structure validation of natural products by quantum-mechanical GIAO calculations of ¹³C NMR chemical shifts. *Chem. Eur. J.* **2002**, *8*, 3233–3239. [[CrossRef](#)]
44. Barone, G.; Duca, D.; Silvestri, A.; Gomez-Paloma, L.; Riccio, R.; Bifulco, G. Determination of the Relative Stereochemistry of Flexible Organic Compounds by Ab Initio Methods: Conformational Analysis and Boltzmann-Averaged GIAO ¹³C NMR Chemical Shifts. *Chem. Eur. J.* **2002**, *8*, 3240–3245. [[CrossRef](#)]
45. Smith, S.G.; Goodman, J.M. Assigning the Stereochemistry of Pairs of Diastereoisomers Using GIAO NMR Shift Calculation. *J. Org. Chem.* **2009**, *74*, 4597–4607. [[CrossRef](#)] [[PubMed](#)]
46. Smit, S.G.; Goodman, J.M. Assigning Stereochemistry to Single Diastereoisomers by GIAO NMR Calculation: The DP4 Probability. *J. Am. Chem. Soc.* **2010**, *132*, 12957–12959. [[CrossRef](#)]
47. Van der Westhuizen, J.H. 'n Nuwe Reeks Fotochemiese Reaksies in Flavonoïedsintese. Ph.D. Thesis, University of the Free State, Bloemfontein, South Africa, 1979.

Sample Availability: Samples of all of the compounds are available from the corresponding author.

Publisher's Note: MDPI stays neutral with regard to jurisdictional claims in published maps and institutional affiliations.



© 2020 by the authors. Licensee MDPI, Basel, Switzerland. This article is an open access article distributed under the terms and conditions of the Creative Commons Attribution (CC BY) license (<http://creativecommons.org/licenses/by/4.0/>).